MULTIPLE SOLUTIONS AND SIMULATIONS FOR AN ION FLOW FIELD PROBLEM APPLIED TO HVDC TRANSMISSION LINES

MADELINE CHAUVIER, SERGE NICAISE, CHRISTOPHE TROESTLER, AND JULIETTE VENEL

ABSTRACT. This paper initiates a mathematical investigation of a PDE model for the transport of high voltage direct current via overhead lines. We prove the existence of infinitely many solutions, give necessary conditions for existence, explicitly compute the continuum of all radial solutions, and develop a new numerical algorithm for this problem.

1. INTRODUCTION

Nowadays, electricity is predominantly transmitted over high-voltage (HV) lines using alternating current (AC) rather than direct current (DC). This is because AC power transmission makes it easy to change the voltage magnitude from low (for electricity usage) to high (for electricity transportation) voltages using transformers. Transporting electricity at a high voltage minimizes energy loss due to Joule heating. However, recent advances in power electronics as well as the development of renewable energies has sparked interest in HVDC transmission. In addition, HVDC has many advantages over HVAC, some of which are highlighted hereafter (for a more thorough discussion, the reader is referred to [14, 15, 25]). Firstly, the DC is more suitable than AC for long-distance transmission overhead lines thanks to lower energy losses. Indeed, the longer the overhead lines, the more reactive power is emitted. The reactive power, which is a parasitic effect specific to AC systems, limits the capacity to transmit active power—the real quantity of interest. In DC systems, this parasitic effect no longer exists. Consequently, the transmission with DC on overhead lines is also more economical after the break-even distance (which is approximately 600–800 km), even if one takes into account the converter station for DC. Secondly, DC is also preferable for underground and submarine lines—such as those bringing the energy from off-shore wind turbines—due to the higher capacitance that affects the transmission when using AC [2]. The cost is lower after 40 km, even when, again, the cost of the DC converter station is taken into account. These advantages are very interesting for transporting renewable energy produced off-shore or at great distances from cities. Finally, and particularly relevant to this paper, the corona effect—whereby some space charges are created—is greatly reduced with DC [24]. However, this last effect also presents some challenges. For overhead lines, the ions migrate away from

Date: November 25, 2025.

2020 *Mathematics Subject Classification.* 35Q60,35G60,35M32,35A16.

Key words and phrases. Ion flow field, HVDC lines, Nonlinear boundary value problems.

the cables due to the fixed polarity of DC, which modifies the electric field in the air up to the ground. For public health reasons, it is important to quantify the magnitude of the electric field on the ground to ensure that it is under an acceptable level.

This subject has already been studied for a couple of years now by several researchers [8, 18, 26] but, as far as we know, it has not been investigated from a mathematical point of view.

The simplest mathematical model used by the engineering community [9, 3, 4, 11] is described by the following three equations in the unipolar case (i.e., for a single conductor).

(1) Poisson's equation:
$$-\Delta\varphi = \frac{\rho}{\varepsilon_0},$$
where φ represents the electric potential, ρ denotes the space charges density and ε_0 is the permittivity of the air.

(2) Ion current equation:
$$J = \big(-\mu\nabla\varphi + W\big)\rho - D\nabla\rho,$$
where J represents the ion current density, and μ, W and D are constants representing respectively the ion mobility, the velocity of the wind, and the diffusion coefficient.

(3) Current continuity equation:
$$\operatorname{div} J = 0.$$

These equations are considered on a domain Ω, which corresponds to the air surrounding the conductors above the ground. Ideally, it would be unbounded, but for practical reasons it is reduced to a bounded domain in a plane orthogonal to the transmission line; see Figure 1 for an illustration.

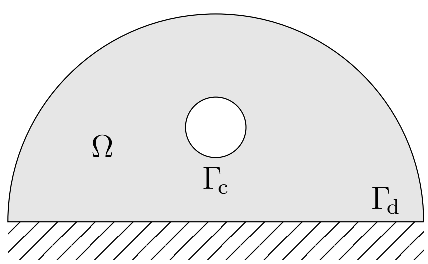

FIGURE 1. A half-disc with a circular conductor.

To maintain a certain degree of generality, we assume that the domain Ω is a bounded and connected set of $\mathbb{R}^2$ such that $\partial\Omega = \Gamma_{\mathrm{c}} \cup \Gamma_{\mathrm{d}}$ and $\Gamma_{\mathrm{c}} \cap \Gamma_{\mathrm{d}} = \varnothing$, Γ_{c} representing the boundary of the conductor, and Γ_{d} the boundary of the air region and the contact with the ground (see Figure 2 for an illustration). We here assume that Γ_{c} is $\mathcal{C}^{1,1}$, while Γ_{d} is a curvilinear polygon of class $\mathcal{C}^{1,1}$ (see [6, Definition 1.4.5.1]) with no re-entrant corner in the sense that $\Gamma_{\mathrm{d}} = \bigcup_{i=1}^{I} \Gamma_{\mathrm{d},i}$, $I \in \mathbb{N}^{\geqslant 1}$, and $\Gamma_{\mathrm{d},i}$ is $\mathcal{C}^{1,1}$ with the interior angle between two consecutive $\Gamma_{\mathrm{d},i}$ is less than π. For simplicity, we consider $W = D = 0$. In addition, without loss of generality, we can normalize the following constants: $\varepsilon_0 = \mu = 1$. With these choices, the previous equations become:

$$\begin{cases} -\Delta\varphi = \rho, & \text{in } \Omega, \\ \operatorname{div}\big(\rho\nabla\varphi\big) = 0, & \text{in } \Omega, \end{cases} \tag{1.1}$$

where φ and ρ are the unknowns defined in the domain Ω.

To solve this problem, we need to add some boundary conditions. It is standard practice [9, 3, 4, 11] to set the potential φ to a constant V on the conductor and to 0 on the ground. Without loss of generality, we can set the potential to 1 on the conductor. To represent the corona effect, physicists commonly fix the outer normal derivative of the potential on the conductor to a function $A : \Gamma_\mathrm{c} \to \mathbb{R}$. This is called the Kaptzov's assumption [8, 10, 17]. The boundary conditions are thus given by:

$$\begin{cases} \varphi = 1, & \text{on } \Gamma_\mathrm{c}, \\ \varphi = 0, & \text{on } \Gamma_\mathrm{d}, \\ \dfrac{\partial\varphi}{\partial\boldsymbol{n}} = A, & \text{on } \Gamma_\mathrm{c}. \end{cases} \tag{1.2}$$

Let us note that no boundary condition is imposed on ρ, one is imposed on φ on Γ_d, and two are imposed on φ on Γ_c. Altogether, this yields three boundary conditions on φ. This can be explained by the fact that using the first equation to eliminate ρ in the second one of (1.1) yields $\operatorname{div}\big((\Delta\varphi)\nabla\varphi\big) = 0$, in Ω, which is a nonlinear partial differential equation of order three in φ.

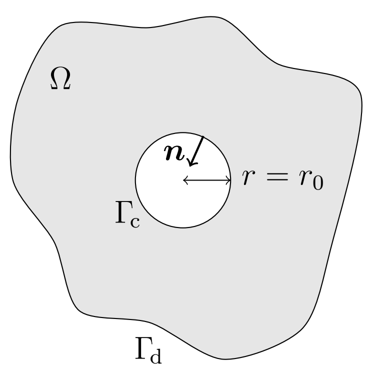

FIGURE 2. A domain Ω around a circular conductor.

A trivial solution to Problem (1.1)–(1.2) for a suitably chosen function A is the *electrostatic solution*, which corresponds to the case of a vanishing charge density, i.e. $\rho \equiv 0$. We denote the corresponding potential φ_e, that is the unique solution to

$$\begin{cases} -\Delta\varphi_\mathrm{e} = 0, & \text{in } \Omega, \\ \varphi_\mathrm{e} = 1, & \text{on } \Gamma_\mathrm{c}, \\ \varphi_\mathrm{e} = 0, & \text{on } \Gamma_\mathrm{d}. \end{cases} \tag{1.3}$$

The aim of this paper is to initiate a mathematical investigation of Problem (1.1)–(1.2) for $\rho \geqslant 0$ and $\rho \not\equiv 0$. In section 2, we use a fixed point argument to prove the existence of a solution with an additional small diffusion term (which is present in some physical models [1, 17, 20, 27]) and with the Neumann condition from (1.2) replaced by a Dirichlet boundary condition on ρ on the whole boundary $\partial\Omega$. Passing to the limit as the diffusion coefficient tends to zero, we show in section 3 the existence of infinitely many solutions (φ, ρ), with $\rho \not\equiv 0$, to problem (1.1) with the Dirichlet boudary conditions from (1.2). However, the Neumann condition from (1.2) is again omitted and, by this limit procedure, the Dirichlet boundary condition on ρ is lost. In section 4, we first use the maximum principle to establish some comparison between the normal derivatives of the solution to (1.1) with the Dirichlet boundary conditions from (1.2) and of the electrostatic solution. We also give bounds on the normal derivative of the electrostatic solution φ_{e} in the particular case where Γ_{c} is circular. This enables us to deduce some necessary conditions on A for a solution to (1.1)–(1.2) to exist. In section 5, we explicitly determine all radial solutions to (1.1)–(1.2) when Ω is an annulus and A is radial (whence constant). Some of these solutions were already mentioned without proof in the electrical engineering community [7, 18, 21, 22] who used them as a benchmark for their algorithms. We also do the same in section 6 to provide evidence for the convergence of a proposed new numerical algorithm.

To conclude this introduction, let us introduce some notation used throughout the paper. The usual norm and semi-norm of $H^s(\Omega)$, $s \geqslant 0$, are denoted by $\|\cdot\|_{s,\Omega}$ and $|\cdot|_{s,\Omega}$, respectively. For $s = 0$ we drop the index s. The scalar product in $L^2(\Omega)$ is denoted by $(\cdot \mid \cdot)_\Omega$. The same notation will be used for vector valued functions. The Fréchet differential of a function J of the variable ρ at a point ρ_0 in the direction z is denoted by $(\partial J/\partial\rho)(\rho_0)[z]$. Finally, $X \hookrightarrow Y$ means that the Banach space X is continuously embedded into the Banach space Y. For the curvilinear polygon $\Gamma_{\mathrm{d}} = \bigcup_{i=1}^{I} \Gamma_{\mathrm{d},i}$, we denote $W^{2-1/p,p}(\Gamma_{\mathrm{d}})$ with $p > 2$ the space of all continuous functions u defined on Γ_{d} such that $u|_{\Gamma_{\mathrm{d},i}} \in W^{2-1/p,p}(\Gamma_{\mathrm{d},i})$ for all i (see [6, Theorem 1.5.2.8] for the general compatibility conditions).

2. Existence of a solution for the unipolar case with diffusion

To prove an existence result for the problem (1.1) with the Dirichlet boundary conditions from (1.2), we first add a diffusion term to regularize the problem. In that case, inspired from existence results for the drift diffusion model (see [13, § 3.2] for instance), using a fixed point argument, an existence result is available.

Theorem 2.1. *Let $\rho_{\mathrm{c}} \in H^{1/2}(\Gamma_{\mathrm{c}})$, $\rho_{\mathrm{d}} \in H^{1/2}(\Gamma_{\mathrm{d}})$, $\rho_{\mathrm{c}}, \rho_{\mathrm{d}} \geqslant 0$ and define $K_+ := \max\{\sup_{\Gamma_{\mathrm{c}}} \rho_{\mathrm{c}}, \sup_{\Gamma_{\mathrm{d}}} \rho_{\mathrm{d}}\}$ which is supposed to be strictly positive. Let us introduce*

$$W := \{\rho \in L^2(\Omega) \mid 0 \leqslant \rho \leqslant K_+\}.$$

Then for all $\varepsilon > 0$, there exists a solution $(\varphi_\varepsilon, \rho_\varepsilon) \in H^2(\Omega) \times \big(W \cap H^1(\Omega)\big)$ to

$$\begin{cases} -\Delta\varphi_\varepsilon = \rho_\varepsilon, & \text{in } \Omega, \\ \operatorname{div}\big(\varepsilon\nabla\rho_\varepsilon + \rho_\varepsilon\nabla\varphi_\varepsilon\big) = 0, & \text{in } \Omega, \\ \varphi_\varepsilon = 1, & \text{on } \Gamma_\mathrm{c}, \\ \varphi_\varepsilon = 0, & \text{on } \Gamma_\mathrm{d}, \\ \rho_\varepsilon = \rho_\mathrm{c}, & \text{on } \Gamma_\mathrm{c}, \\ \rho_\varepsilon = \rho_\mathrm{d}, & \text{on } \Gamma_\mathrm{d}. \end{cases} \tag{2.1}$$

Moreover, $\varphi_\varepsilon \in W^{2,q}(\Omega)$ for every $q \geqslant 2$. Finally, if $\rho_\mathrm{c} \in W^{2-1/p,p}(\Gamma_\mathrm{c})$ and $\rho_\mathrm{d} \in W^{2-1/p,p}(\Gamma_\mathrm{d})$ for some $p > 2$, then $\rho_\varepsilon \in W^{2,p}(\Omega)$.

The idea of the proof is to transform System (2.1) into a fixpoint $\rho = G(\rho)$ by splitting it into two simpler equations. More precisely, given $\rho_0 \in W$, solve

$$\begin{cases} -\Delta\varphi = \rho, & \text{in } \Omega, \\ \varphi = 1, & \text{on } \Gamma_\mathrm{c}, \\ \varphi = 0, & \text{on } \Gamma_\mathrm{d}, \end{cases} \tag{2.2}$$

with $\rho = \rho_0$ for the unknown is φ, and with that solution φ_0 solve

$$\begin{cases} \operatorname{div}\big(\varepsilon\nabla\rho_1 + \rho_1\nabla\varphi_0\big) = 0, & \text{in } \Omega, \\ \rho_1 = \rho_\mathrm{c}, & \text{on } \Gamma_\mathrm{c}, \\ \rho_1 = \rho_\mathrm{d}, & \text{on } \Gamma_\mathrm{d}, \end{cases} \tag{2.3}$$

for ρ_1. Set $G(\rho_0) \coloneqq \rho_1$.

Before detailing the proof of Theorem 2.1, let us start with a few preparation lemmas.

Lemma 2.2. *The linear map $W \to H^1(\Omega) : \rho \mapsto \varphi$ where φ is the unique solution to (2.2) is well defined and continuous from W endowed with the L^2-topology to $W^{2,q}(\Omega)$ for any $q \geqslant 2$. Moreover its image is bounded in the sense that, there exists positive constants C_q, for every $q \geqslant 2$, and C_∞ such that, for all φ in the image, $\varphi \in C^1(\overline{\Omega})$,*

$$\|\varphi\|_{W^{2,q}(\Omega)} \leqslant C_q, \quad \textit{and} \tag{2.4}$$

$$\|\nabla\varphi\|_{L^\infty(\Omega;\mathbb{R}^2)} \leqslant C_\infty. \tag{2.5}$$

The proof of this statement is quite standard but we sketch it briefly for the reader's convenience.

Proof. Thanks to [6, Theorem 5.2.7], there exists a unique $\varphi \in H^2(\Omega)$ satisfying (2.2). Furthermore as $\rho \in L^\infty(\Omega)$, we also have $\varphi \in W^{2,q}(\Omega)$ for every $q \geqslant 2$. As a consequence, the electrostatic solution $\varphi_\mathrm{e} \in H^1(\Omega)$ defined by (1.3) also belongs to $W^{2,q}(\Omega)$, for all $q \geqslant 2$. Hence the difference $\varphi - \varphi_\mathrm{e}$ satisfies

$$\begin{cases} -\Delta(\varphi - \varphi_\mathrm{e}) = \rho, & \text{in } \Omega, \\ \varphi - \varphi_\mathrm{e} = 0, & \text{on } \partial\Omega = \Gamma_\mathrm{c} \cup \Gamma_\mathrm{d}. \end{cases}$$

Thus there exists a constant $\tilde{C}_q > 0$ such that

$$\|\varphi - \varphi_{\mathrm{e}}\|_{W^{2,q}(\Omega)} \leqslant \tilde{C}_q \|\rho\|_{L^q(\Omega)} \leqslant \tilde{C}_q K_+ |\Omega|^{1/q},$$

where the last inequality results from the fact that ρ belongs to W. Thus the continuity is established. In addition, estimate (2.4) directly follows from the triangular inequality with $C_q \coloneqq \|\varphi_{\mathrm{e}}\|_{W^{2,q}(\Omega)} + \tilde{C}_q K_+ |\Omega|^{1/q}$.

Finally, from the continuous embedding $W^{2,q}(\Omega) \hookrightarrow \mathcal{C}^1(\overline{\Omega})$ for $q > 2$, we deduce that $\nabla\varphi$ is in $L^\infty(\Omega; \mathbb{R}^2)$ with

$$\|\nabla\varphi\|_{L^\infty(\Omega;\mathbb{R}^2)} \leqslant C_\infty \coloneqq K_q C_q, \tag{2.6}$$

where K_q is the norm of the embedding of $W^{2,q}(\Omega)$ into $\mathcal{C}^1(\overline{\Omega})$. □

Lemma 2.3. *Under the assumptions of Theorem 2.1, for $\rho_0 \in W$, there exists a unique solution $\rho_1 \in W \cap H^1(\Omega)$ to (2.3) with φ_0 a solution to (2.2). Moreover, if $\rho_{\mathrm{c}} \in W^{2-1/p,p}(\Gamma_{\mathrm{c}})$ and $\rho_{\mathrm{d}} \in W^{2-1/p,p}(\Gamma_{\mathrm{d}})$ for some $p > 2$, then $\rho_1 \in W^{2,p}(\Omega)$.*

Proof. We are looking for a solution ρ_1 of (2.3). Due to the non homogeneous boundary conditions, we first consider a lifting $r \in H^1(\Omega)$ of the boundary data [6, Theorem 1.5.1.3], namely such that

$$\begin{cases} r = \rho_{\mathrm{c}}, & \text{on } \Gamma_{\mathrm{c}}, \\ r = \rho_{\mathrm{d}}, & \text{on } \Gamma_{\mathrm{d}}. \end{cases} \tag{2.7}$$

Now, we are looking for $\tilde{\rho}_1 \coloneqq \rho_1 - r$ in $H^1_0(\Omega)$ which satisfies

$$\operatorname{div}\big(\varepsilon\nabla\tilde{\rho}_1 + \tilde{\rho}_1\nabla\varphi_0\big) = -\operatorname{div}\big(\varepsilon\nabla r + r\nabla\varphi_0\big), \text{ in } \Omega, \tag{2.8}$$

or in the variational form

$$\forall\chi \in H^1_0(\Omega), \quad \int_\Omega \big(\varepsilon\nabla\tilde{\rho}_1 + \tilde{\rho}_1\nabla\varphi_0\big)\nabla\chi \,\mathrm{d}x = -\int_\Omega \big(\varepsilon\nabla r + r\nabla\varphi_0\big)\nabla\chi \,\mathrm{d}x. \tag{2.9}$$

We assert that the bilinear form a defined by

$$a : H^1_0(\Omega) \times H^1_0(\Omega) \to \mathbb{R} : (\rho, \chi) \mapsto \int_\Omega \big(\varepsilon\nabla\rho + \rho\nabla\varphi_0\big)\nabla\chi \,\mathrm{d}x, \tag{2.10}$$

is continuous and coercive. Indeed, the continuity stems from Cauchy-Schwarz's inequality by using $\nabla\varphi_0 \in W^{1,q}(\Omega; \mathbb{R}^2)$ and the continuous embedding $W^{1,q}(\Omega; \mathbb{R}^2) \hookrightarrow \mathcal{C}(\bar{\Omega}; \mathbb{R}^2)$ for $q > 2$. Furthermore, by Green's formula, for $\chi \in H^1_0(\Omega)$, we have

$$\begin{aligned} \int_\Omega \chi\nabla\varphi_0\nabla\chi \,\mathrm{d}x &= -\int_\Omega \operatorname{div}\big(\chi\nabla\varphi_0\big)\chi \,\mathrm{d}x \\ &= -\int_\Omega \nabla\chi\nabla\varphi_0\chi \,\mathrm{d}x - \int_\Omega \chi^2\Delta\varphi_0 \,\mathrm{d}x. \end{aligned}$$

Since $-\Delta\varphi_0 = \rho_0$, it follows that

$$2\int_\Omega \chi\nabla\varphi_0\nabla\chi \,\mathrm{d}x = \int_\Omega \chi^2\rho_0 \,\mathrm{d}x \geqslant 0.$$

So

$$a(\chi,\chi) = \int_\Omega \varepsilon|\nabla\chi|^2 + \tfrac{1}{2}\rho_0\chi^2 \,\mathrm{d}x. \tag{2.11}$$

Therefore a is coercive in $H_0^1(\Omega)$ and, thanks to the Lax-Milgram theorem, there exists a unique solution $\tilde{\rho}_1 \in H_0^1(\Omega)$ of (2.9). Hence, we also conclude that there exists a unique $\rho_1 \in H^1(\Omega)$ solution of (2.3).

We also need to show that $\rho_1 \in W$. Notice that we can apply the maximum principle [5, Theorem 8.1] to the system (2.3) because $\operatorname{div}\nabla\varphi_0 = -\rho_0 \leqslant 0$ (see condition 8.8 in [5]). Therefore

$$0 \leqslant \rho_1 \leqslant K_+,$$

because $\rho_{\mathrm{c}}^- = \rho_{\mathrm{d}}^- = 0$. Thus $\rho_1 \in W \cap H^1(\Omega)$.

Now let us assume that $\rho_{\mathrm{c}} \in W^{2-1/p,p}(\Gamma_{\mathrm{c}})$ and $\rho_{\mathrm{d}} \in W^{2-1/p,p}(\Gamma_{\mathrm{d}})$ for some $p > 2$ and show that $\rho_1 \in W^{2,p}(\Omega)$. First note that one can choose $r \in W^{2,p}(\Omega) \hookrightarrow H^2(\Omega)$ (see [6, Theorem 1.5.2.8] where it is standard that the compatibility conditions can be satisfied with a suitable choice of the normal derivative on the boundary Γ_{d}). Expanding (2.8) and using that $-\Delta\varphi_0 = \rho_0$ yields

$$\operatorname{div}(\varepsilon\nabla\tilde{\rho}_1) = \tilde{\rho}_1\rho_0 - \nabla\tilde{\rho}_1\nabla\varphi_0 - \varepsilon\Delta r - \nabla r\nabla\varphi_0 + r\rho_0. \tag{2.12}$$

Since $\nabla\varphi_0 \in L^\infty(\Omega;\mathbb{R}^2)$ and $\rho_0 \in L^\infty(\Omega)$, we deduce from (2.12) that $\Delta\tilde{\rho}_1 \in L^2(\Omega)$ and so $\tilde{\rho}_1 \in H^2(\Omega)$ with the help of [6, Theorem 5.2.7]. Due to the continuous embedding $H^1(\Omega;\mathbb{R}^2) \hookrightarrow L^p(\Omega;\mathbb{R}^2)$, $\nabla\tilde{\rho}_1 \in L^p(\Omega;\mathbb{R}^2)$. Therefore, Equality (2.12) implies that $\Delta\tilde{\rho}_1 \in L^p(\Omega)$ and so that $\tilde{\rho}_1 \in W^{2,p}(\Omega)$, again by [6, Theorem 5.2.7]. Thus $\rho_1 \in W^{2,p}(\Omega)$. □

Lemma 2.4. *Under the assumptions of Theorem 2.1, the functional G is completely continuous from W to W.*

Proof. Let $(\rho_{0,n})_{n\in\mathbb{N}}$ be a bounded sequence included in W. For every n, let $\varphi_{0,n}$ be the solution to (2.2) with $\rho_{0,n}$ instead of ρ and $\rho_{1,n} = G(\rho_{0,n})$ be the solution to (2.3) with $\varphi_{0,n}$ instead of φ_0. Let us prove that, up to a subsequence, $(\rho_{1,n})_n$ strongly converges in W.

First, there exists a subsequence of $(\rho_{0,n})_n$, still denoted by $(\rho_{0,n})_n$, and $\rho_0 \in L^2(\Omega)$ such that

$$\rho_{0,n} \rightharpoonup \rho_0 \quad \text{weakly in } L^2(\Omega),$$

with $\rho_0 \in W$ since W is convex, whence weakly closed.

Secondly, Lemma 2.2 implies that the sequence $(\varphi_{0,n})_n$ is bounded in $H^2(\Omega)$. Hence by the compact embedding of $H^2(\Omega)$ into $H^s(\Omega)$, for any $s \in [0,2[$, passing if necessary to a subsequence, there exists $\varphi_0 \in H^s(\Omega)$, such that

$$\varphi_{0,n} \to \varphi_0 \quad \text{strongly in } H^s(\Omega) \text{ for all } s \in [0,2[. \tag{2.13}$$

Using the variational formulation of (2.2), we deduce that φ_0 is solution of (2.2) with $\rho = \rho_0$ and Lemma 2.2 implies that $\|\nabla\varphi_0\|_{L^\infty(\Omega;\mathbb{R}^2)} \leqslant C_\infty$.

Thirdly, let $\tilde{\rho}_{1,n} \coloneqq \rho_{1,n} - r$ for every $n \in \mathbb{N}$ where $r \in H^1_0(\Omega)$ is defined by (2.7). In (2.9), with $\tilde{\rho}_{1,n}$ and $\chi = \tilde{\rho}_{1,n}$, we will have, thanks to Cauchy-Schwarz's inequality, (2.11) and (2.5),

$$\begin{aligned}\varepsilon \int_\Omega |\nabla \tilde{\rho}_{1,n}|^2 \,\mathrm{d}x \leqslant a(\tilde{\rho}_{1,n}, \tilde{\rho}_{1,n}) &= - \int_\Omega \big(\varepsilon \nabla r + r \nabla \varphi_{0,n}\big) \nabla \tilde{\rho}_{1,n} \,\mathrm{d}x \\ &\leqslant \varepsilon \|\nabla r\|_\Omega \, \|\nabla \tilde{\rho}_{1,n}\|_\Omega + C_\infty \|r\|_\Omega \|\nabla \tilde{\rho}_{1,n}\|_\Omega.\end{aligned}$$

Therefore, $(\tilde{\rho}_{1,n})_n$ is bounded in $H^1_0(\Omega)$, thus, up to a subsequence, there exists $\tilde{\rho}_1 \in H^1_0(\Omega)$,

$$\tilde{\rho}_{1,n} \rightharpoonup \tilde{\rho}_1 \quad \text{weakly in } H^1_0(\Omega),$$

and

$$\tilde{\rho}_{1,n} \to \tilde{\rho}_1 \quad \text{strongly in } H^t(\Omega), \text{ for all } t \in [0,1[. \tag{2.14}$$

To show that ρ_1 is a solution of (2.3), let us establish that $\tilde{\rho}_1$ is solution of (2.9). We know that

$$\forall \chi \in H^1_0(\Omega), \quad \int_\Omega \big(\varepsilon \nabla \tilde{\rho}_{1,n} + \tilde{\rho}_{1,n} \nabla \varphi_{0,n}\big) \nabla \chi \,\mathrm{d}x = - \int_\Omega \big(\varepsilon \nabla r + r \nabla \varphi_{0,n}\big) \nabla \chi \,\mathrm{d}x. \tag{2.15}$$

But, by (2.13) and (2.14) and the help of [6, Theorem 1.4.4.2], we deduce that

$$\tilde{\rho}_{1,n} \nabla \varphi_{0,n} \to \tilde{\rho}_1 \nabla \varphi_0 \quad \text{strongly in } L^2(\Omega; \mathbb{R}^2).$$

Consequently, because $(\tilde{\rho}_{1,n})_n$ converges weakly in $H^1_0(\Omega)$ to $\tilde{\rho}_1$ and $(\varphi_{0,n})_n$ converges strongly to φ_0 in $H^1(\Omega)$, it is possible to take the limit in equation (2.15) . Therefore, we deduce that $(\rho_{1,n})_n$ strongly converges in $L^2(\Omega)$ to $\rho_1 = \tilde{\rho}_1 + r = G(\rho_0) \in W$ solution of (2.3). By Lemma 2.3, we also have $\rho_1 \in W^{2,p}(\Omega) \cap W$. □

Proof of Theorem 2.1. As mentioned previously, we are using a fixed point argument to solve this system. To this end, we first split it into two subsystems. Given $\rho_0 \in W$, we successively solve (2.2) with $\rho = \rho_0$ to get φ_0 and then (2.3) for ρ_1 and define $G(\rho_0) \coloneqq \rho_1$.

The existence and regularity of φ_0 is given by Lemma 2.2. Given such a φ_0, Lemma 2.3 implies that Problem (2.3) has a unique solution $\rho_1 \in H^1(\Omega) \cap W$ and thanks to Lemma 2.4, G is completely continuous from W to W. Hence by Schauder's fixed point theorem [28, Theorem 1.2.3], G has a fixed point in W. In other words, there exists a solution $(\varphi_\varepsilon, \rho_\varepsilon)$ of (2.1) with $\varphi_\varepsilon \in W^{2,q}(\Omega)$ for every $q \geqslant 2$ and $\rho_\varepsilon \in W \cap H^1(\Omega)$.

Finally, if $\rho_\mathrm{c} \in W^{2-1/p,p}(\Gamma_\mathrm{c})$ and $\rho_\mathrm{d} \in W^{2-1/p,p}(\Gamma_\mathrm{d})$, Lemma 2.3 gives the desired regularity on ρ_ε. □

3. Existence of infinitely many solutions in a unipolar case

Thanks to Theorem 2.1 of the previous section we can show the existence of a nontrivial solution (φ, ρ) to the following system:

$$\begin{cases} -\Delta\varphi = \rho, & \text{in } \Omega, \\ \operatorname{div}(\rho\nabla\varphi) = 0, & \text{in } \Omega, \\ \varphi = 1, & \text{on } \Gamma_{\mathrm{c}}, \\ \varphi = 0, & \text{on } \Gamma_{\mathrm{d}}. \end{cases} \tag{3.1}$$

Note that this system is not exactly the one we want to solve because it does not contain the Neumann boundary condition (see the boundary conditions (1.2) in the introduction). But once a solution (φ, ρ) of (3.1) is known, we can say that it is a solution of (1.1)–(1.2) for some A being given by $\partial\varphi/\partial\boldsymbol{n}$ (a non-constant function in general).

Theorem 3.1. *Problem* (3.1) *possesses infinitely many nontrivial solutions. More precisely, for all* $n \in \mathbb{N}$*, there exists a solution* $(\varphi_n^*, \rho_n^*) \in H^2(\Omega) \times W$ *to* (3.1) *with* $\rho_n^* \not\equiv 0$*,* $\varphi_n^* \in W^{2,q}(\Omega)$ *for every* $q > 2$*, and* $\|\rho_n^*\|_{L^\infty(\Omega)} \xrightarrow[n\to\infty]{} 0$.

Proof. Let us first show the existence of one nontrivial solution. For every positive integer ℓ, let us denote by $(\varphi_\ell, \rho_\ell)$ a solution given by Theorem 2.1 for $\varepsilon = 1/\ell$, $\rho_{\mathrm{c}}(x) = \hat{\rho}_{\mathrm{c}}$ where $\hat{\rho}_{\mathrm{c}} > 0$ is a fixed constant, and $\rho_{\mathrm{d}} \equiv 0$. Note that $K_+ = \hat{\rho}_{\mathrm{c}}$. Because $(\rho_\ell)_\ell \subseteq W$, it is bounded in $L^2(\Omega)$, so, going if necessary to a subsequence, there exists $\rho \in L^2(\Omega)$ such that

$$\rho_\ell \rightharpoonup \rho \quad \text{weakly in } L^2(\Omega), \quad \text{as } \ell \to +\infty. \tag{3.2}$$

Note that $\rho \in W$. Lemma 2.2 implies that $\varphi_\ell \rightharpoonup \varphi$ weakly in $W^{2,q}(\Omega)$ for all $q \geqslant 2$. Therefore, for any $s \in [0, 2[$, $(\varphi_\ell)_\ell$ converges strongly to φ in $H^s(\Omega)$ whenever $\ell \to \infty$. In particular, $\nabla\varphi_\ell \to \nabla\varphi$ in $L^2(\Omega; \mathbb{R}^2)$. As in the proof of Lemma 2.4, we can deduce that φ is the solution to (2.2).

Now, let us prove that $\operatorname{div}(\rho\nabla\varphi) = 0$. For any fixed $\chi \in L^2(\Omega)$, we have

$$\big(\rho_\ell\nabla\varphi_\ell - \rho\nabla\varphi \bigm| \chi\big)_\Omega = \big(\rho_\ell(\nabla\varphi_\ell - \nabla\varphi) \bigm| \chi\big)_\Omega + \big((\rho_\ell - \rho)\nabla\varphi \bigm| \chi\big)_\Omega.$$

The first term tends to 0 because

$$\big|(\rho_\ell(\nabla\varphi_\ell - \nabla\varphi)|\chi)_\Omega\big| \leqslant K_+\|\nabla\varphi_\ell - \nabla\varphi\|_\Omega\|\chi\|_\Omega \xrightarrow[\ell\to\infty]{} 0.$$

In addition, since $\nabla\varphi \in W^{1,q}(\Omega; \mathbb{R}^2) \hookrightarrow L^\infty(\Omega; \mathbb{R}^2)$, for $q > 2$, we have $\chi\nabla\varphi \in L^2(\Omega; \mathbb{R}^2)$. From (3.2), we deduce that the second term also tends to 0. In other words

$$\rho_\ell\nabla\varphi_\ell \rightharpoonup \rho\nabla\varphi \quad \text{weakly in } L^2(\Omega; \mathbb{R}^2). \tag{3.3}$$

Since $(\varphi_\ell, \rho_\ell)$ is a solution to (2.1), we have for all $\chi \in \mathcal{D}(\Omega)$ [1],

$$0 = \big(\tfrac{1}{\ell}\nabla\rho_\ell + \rho_\ell\nabla\varphi_\ell \bigm| \nabla\chi\big)_\Omega = -\tfrac{1}{\ell}\big(\rho_\ell \bigm| \Delta\chi\big)_\Omega + \big(\rho_\ell\nabla\varphi_\ell \bigm| \nabla\chi\big)_\Omega.$$

[1] $\mathcal{D}(\Omega)$ is the set of smooth functions with a compact support included in Ω.

Moreover, $\frac{1}{\ell}(\rho_\ell|\Delta\chi)_\Omega$ tends to 0 because $(\rho_\ell)_\ell$ is bounded in $L^2(\Omega)$ and $\Delta\chi \in L^2(\Omega)$. So we deduce

$$\big(\rho_\ell \nabla\varphi_\ell \bigm| \nabla\chi\big)_\Omega \to 0.$$

And so, by the uniqueness of the limit, and with (3.3), $(\rho\nabla\varphi|\nabla\chi)_\Omega = 0$ for every $\chi \in \mathcal{D}(\Omega)$. This implies $\operatorname{div}(\rho\nabla\varphi) = 0$ in the sense of distributions.

Consequently (φ, ρ) is a solution of (3.1).

In order to justify that the solution (φ, ρ) is different from the trivial solution $(\varphi_{\mathrm{e}}, 0)$ defined by (1.3), it remains to show that $\rho \not\equiv 0$. Since $0 \leqslant \rho_\ell \leqslant K_+ = \hat\rho_{\mathrm{c}}$ a.e. in Ω, $\partial\rho_\ell/\partial\boldsymbol{n} \geqslant 0$ on Γ_{c}.

Let us fix $\chi \in H^2(\Omega)$ such that $\chi \geqslant 0$ on Γ_{c} and $\chi \equiv 0$ on Γ_{d}. So

$$\begin{aligned}
0 &= \int_\Omega \operatorname{div}\big(\tfrac{1}{\ell}\nabla\rho_\ell + \rho_\ell\nabla\varphi_\ell\big)\chi\,\mathrm{d}x\\
&= -\int_\Omega \big(\tfrac{1}{\ell}\nabla\rho_\ell + \rho_\ell\nabla\varphi_\ell\big)\nabla\chi\,\mathrm{d}x + \int_{\Gamma_{\mathrm{c}}} \big(\tfrac{1}{\ell}\nabla\rho_\ell\cdot\boldsymbol{n} + \rho_\ell\nabla\varphi_\ell\cdot\boldsymbol{n}\big)\chi\,\mathrm{d}x\\
&= -\int_\Omega \rho_\ell\nabla\varphi_\ell\nabla\chi\,\mathrm{d}x + \frac{1}{\ell}\int_\Omega \rho_\ell\Delta\chi\,\mathrm{d}x - \frac{1}{\ell}\int_{\partial\Omega}\rho_\ell\frac{\partial\chi}{\partial\boldsymbol{n}}\,\mathrm{d}x + \int_{\Gamma_{\mathrm{c}}}\Big(\frac{1}{\ell}\frac{\partial\rho_\ell}{\partial\boldsymbol{n}} + \hat\rho_{\mathrm{c}}\frac{\partial\varphi_\ell}{\partial\boldsymbol{n}}\Big)\chi\,\mathrm{d}x.
\end{aligned}$$

Using $\partial\rho_\ell/\partial\boldsymbol{n} \geqslant 0$ on Γ_{c}, this implies

$$\int_\Omega \rho_\ell\nabla\varphi_\ell\nabla\chi\,\mathrm{d}x \geqslant \frac{1}{\ell}\int_\Omega \rho_\ell\Delta\chi\,\mathrm{d}x - \frac{1}{\ell}\int_{\partial\Omega}\rho_\ell\frac{\partial\chi}{\partial\boldsymbol{n}}\,\mathrm{d}x + \int_{\Gamma_{\mathrm{c}}}\hat\rho_{\mathrm{c}}\frac{\partial\varphi_\ell}{\partial\boldsymbol{n}}\chi\,\mathrm{d}x. \tag{3.4}$$

We want to pass to the limit $\ell \to \infty$ in this inequality. First, since $\int_\Omega \rho_\ell\Delta\chi\,\mathrm{d}x$ tends to $\int_\Omega \rho\Delta\chi\,\mathrm{d}x$, one has

$$\frac{1}{\ell}\int_\Omega \rho_\ell\Delta\chi\,\mathrm{d}x \xrightarrow[\ell\to\infty]{} 0.$$

Secondly, since

$$\int_{\partial\Omega}\rho_\ell\frac{\partial\chi}{\partial\boldsymbol{n}}\,\mathrm{d}x = \int_{\Gamma_{\mathrm{c}}}\hat\rho_{\mathrm{c}}\frac{\partial\chi}{\partial\boldsymbol{n}}\,\mathrm{d}x + \int_{\Gamma_{\mathrm{d}}}\rho_{\mathrm{d}}\frac{\partial\chi}{\partial\boldsymbol{n}}\,\mathrm{d}x$$

is a constant, this implies that

$$\frac{1}{\ell}\int_{\partial\Omega}\rho_\ell\frac{\partial\chi}{\partial\boldsymbol{n}}\,\mathrm{d}x \xrightarrow[\ell\to\infty]{} 0.$$

Moreover, with (3.3) and since $\partial\varphi_\ell/\partial\boldsymbol{n}$ tends to $\partial\varphi/\partial\boldsymbol{n}$ strongly in $L^2(\Gamma_{\mathrm{c}})$, we can pass to the limit in (3.4) and we obtain:

$$\int_\Omega \rho\nabla\varphi\nabla\chi\,\mathrm{d}x \geqslant \int_{\Gamma_{\mathrm{c}}}\hat\rho_{\mathrm{c}}\frac{\partial\varphi}{\partial\boldsymbol{n}}\chi\,\mathrm{d}x.$$

This implies that $\rho \not\equiv 0$. Indeed, if $\rho \equiv 0$, then $\varphi = \varphi_{\mathrm{e}}$ and so we will have

$$0 \geqslant \int_{\Gamma_{\mathrm{c}}}\hat\rho_{\mathrm{c}}\frac{\partial\varphi_{\mathrm{e}}}{\partial\boldsymbol{n}}\chi\,\mathrm{d}x.$$

But $\hat{\rho}_c > 0$ and $\partial\varphi_e/\partial\boldsymbol{n} \geqslant 0$ is non identically zero (thanks to the strong maximum principle), choosing $\chi > 0$ on Γ_c yields the contradiction

$$0 \geqslant \int_{\Gamma_c} \hat{\rho}_c \frac{\partial\varphi_e}{\partial\boldsymbol{n}} \chi \,\mathrm{d}x > 0.$$

So $\rho \not\equiv 0$ and we have proved the existence of a nontrivial solution (φ, ρ) to the system (3.1).

To conclude, let us show the existence of infinitely many solutions. Since $\rho \not\equiv 0$, there exists a positive constant $K_0 \leqslant \hat{\rho}_c$ such that $\|\rho\|_{L^\infty(\Omega)} = K_0$. If we repeat the above argument with $\rho = K_0/2$ on Γ_c and $\rho = 0$ on Γ_d, we obtain the existence of a nontrivial solution (φ_1, ρ_1) to Problem (3.1). The bound $\|\rho_1\|_{L^\infty(\Omega)} \leqslant K_0/2$ implies that $\rho_1 \neq \rho$. We conclude by iterating the above procedure. □

4. Properties on the normal derivative of the solution

In this section, we establish bounds on the normal derivative of solutions to (1.1) in term of the normal derivatives of the electrostatic solution φ_e. We also provide quantitative estimates on the latter in the special case when Γ_c is a circle.

Let us start with a theorem that provides necessary and sufficient conditions on $A = \partial\varphi/\partial\boldsymbol{n}|_{\Gamma_c}$ for a solution of Poisson's equation with a nonnegative right-hand-side to exist.

Theorem 4.1. *Let Ω be an open subset of $\mathbb{R}^2$ satisfying the assumptions of the introduction and $\varphi \in H^1(\Omega)$ be the unique solution of*

$$\begin{cases} -\Delta\varphi = \rho, & \text{in } \Omega, \\ \varphi = 0, & \text{on } \Gamma_d, \\ \varphi = 1, & \text{on } \Gamma_c, \end{cases} \tag{4.1}$$

where $\rho \in L^p(\Omega)$, with $p > 2$ and $\rho \geqslant 0$. Let $\varphi_e \in H^1(\Omega)$ be the solution of (1.3). Then we have

$$\frac{\partial\varphi_e}{\partial\boldsymbol{n}} > 0, \text{ on } \Gamma_c \qquad \text{and} \qquad \frac{\partial\varphi_e}{\partial\boldsymbol{n}} < 0, \text{ on } \Gamma_d \setminus \mathcal{V},$$

where $\mathcal{V}$ is the set of corners of Γ_d. Moreover, the three following properties are equivalent:

$$\rho \not\equiv 0, \tag{4.2}$$

$$\frac{\partial\varphi}{\partial\boldsymbol{n}} < \frac{\partial\varphi_e}{\partial\boldsymbol{n}}, \quad \text{on } \Gamma_c, \tag{4.3}$$

$$\frac{\partial\varphi}{\partial\boldsymbol{n}} < \frac{\partial\varphi_e}{\partial\boldsymbol{n}}, \quad \text{on } \Gamma_d \setminus \mathcal{V}. \tag{4.4}$$

Proof. First, by using the strong maximum principle and the Hopf boundary point lemma to φ_e [5, Theorem 2.2 & Lemma 3.4] (see also [23, Theorem 3.27, Lemma 3.26]), we obtain that $0 < \varphi_e < 1$ and $\partial\varphi_e/\partial\boldsymbol{n} < 0$ on $\Gamma_d \setminus \mathcal{V}$ and $\partial\varphi_e/\partial\boldsymbol{n} > 0$ on Γ_c.

First, assume that (4.2) and prove (4.3) and (4.4). Let us consider $d \coloneqq \varphi - \varphi_{\mathrm{e}}$ which solves

$$\begin{cases} -\Delta d = \rho, & \text{in } \Omega, \\ d = 0, & \text{on } \partial\Omega. \end{cases}$$

As d cannot be 0, thanks to the strong maximum principle, we have

$$d > 0 \text{ in } \Omega.$$

Thus by the Hopf boundary point lemma, we have $\partial d/\partial \boldsymbol{n} < 0$ on $\partial\Omega \setminus \mathcal{V}$, which establishes (4.3) and (4.4).

Now let us prove that (4.3) (resp. (4.4)) implies (4.2). Assume on the contrary that $\rho \equiv 0$. Then, $\varphi = \varphi_{\mathrm{e}}$ contradicting (4.3) (resp. (4.4)). □

Let us now turn to the quantitative estimates on $\partial\varphi_{\mathrm{e}}/\partial\boldsymbol{n}$.

Theorem 4.2. *Assume that* $\Gamma_{\mathrm{c}} = \partial B(0, r_0) \subseteq \mathbb{R}^2$, *for some* $r_0 > 0$ *and let* φ_{e} *be the solution of* (1.3). *Then*

$$\frac{1}{r_0 \ln(r_2/r_0)} \leqslant \frac{\partial \varphi_{\mathrm{e}}}{\partial \boldsymbol{n}}\bigg|_{\Gamma_{\mathrm{c}}} \leqslant \frac{1}{r_0 \ln(r_1/r_0)}, \tag{4.5}$$

where $r_1 = \min_{x\in\Gamma_{\mathrm{d}}} |x|$ *and* $r_2 = \max_{x\in\Gamma_{\mathrm{d}}} |x|$.

Note that $r_2 \geqslant r_1 > r_0$ are such that $B(0, r_1) \subseteq \Omega \subseteq B(0, r_2)$, see Figure 3 for an illustration.

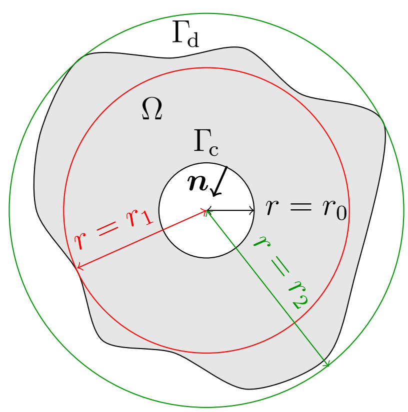

FIGURE 3. A domain with a circular conductor with the inscribed and circumscribed disks.

Proof. For $i \in \{1, 2\}$, let $\varphi_{\mathrm{e}}^{(i)}$ be given by

$$\varphi_{\mathrm{e}}^{(i)}(x) \coloneqq \frac{\ln(r/r_i)}{\ln(r_0/r_i)}. \tag{4.6}$$

We readily check that $\varphi_{\mathrm{e}}^{(i)}$ is the unique solution of

$$\begin{cases} \Delta\varphi_{\mathrm{e}}^{(i)} = 0, & \text{in } B(0,r_i)\backslash B(0,r_0), \\ \varphi_{\mathrm{e}}^{(i)} = 1, & \text{on } \Gamma_{\mathrm{c}}, \\ \varphi_{\mathrm{e}}^{(i)} = 0, & \text{on } \partial B(0,r_i). \end{cases} \tag{4.7}$$

Let us start with the right inequality of (4.5). Thanks to (4.6), we directly see that $\varphi_{\mathrm{e}}^{(1)} \leqslant 0$ on Γ_{d}. Then $d^{(1)} \coloneqq \varphi_{\mathrm{e}} - \varphi_{\mathrm{e}}^{(1)}$ is a solution to

$$\begin{cases} \Delta d^{(1)} = 0, & \text{in } \Omega, \\ d^{(1)} = 0, & \text{on } \Gamma_{\mathrm{c}}, \\ d^{(1)} \geqslant 0, & \text{on } \Gamma_{\mathrm{d}}, \end{cases}$$

and, thanks to the maximum principle [5, Theorem 3.1], $d^{(1)} \geqslant 0$ in Ω. Therefore

$$\left.\frac{\partial d^{(1)}}{\partial \boldsymbol{n}}\right|_{\Gamma_{\mathrm{c}}} \leqslant 0 \qquad \text{i.e.} \qquad \left.\frac{\partial \varphi_{\mathrm{e}}}{\partial \boldsymbol{n}}\right|_{\Gamma_{\mathrm{c}}} \leqslant \left.\frac{\partial \varphi_{\mathrm{e}}^{(1)}}{\partial \boldsymbol{n}}\right|_{\Gamma_{\mathrm{c}}} = \frac{-1}{r_0 \ln(r_0/r_1)}.$$

The same argument implies the left inequality of (4.5) because (4.6) yields $\varphi_{\mathrm{e}}^{(2)} \geqslant 0$ on Γ_{d}. ☐

Remark 4.3. Assuming that $\Gamma_{\mathrm{c}} = \partial B(0,r_0)$, for some $r_0 > 0$, Theorems 4.1 and 4.2 allows us to draw the following two conclusions.

If

$$A = \frac{\partial \varphi}{\partial \boldsymbol{n}} > \frac{1}{r_0 \ln(r_1/r_0)} \text{ on } \Gamma_{\mathrm{c}},$$

then (4.1) has no solution and neither has Problem (1.1)–(1.2).

If

$$A = \frac{\partial \varphi}{\partial \boldsymbol{n}} \leqslant \frac{1}{r_0 \ln(r_2/r_0)} \text{ on } \Gamma_{\mathrm{c}},$$

then a solution to Problem (1.1)–(1.2) *may* exist.

5. Analytical solutions for the unipolar radial case

In this section, we consider a simpler domain Ω. More precisely Ω is supposed to be an annulus (see Figure 4) and is given by $\Omega \coloneqq \big\{(r\cos\theta, r\sin\theta) \in \mathbb{R}^2 \;\big|\; r_0 < r < 1, 0 \leqslant \theta \leqslant 2\pi\big\}$ where $0 < r_0 < 1$.

Here $\Gamma_{\mathrm{c}} = \partial B(0,r_0)$ and $\Gamma_{\mathrm{d}} = \partial B(0,1)$. Our aim is to compute all the radial solutions to (1.1)–(1.2), that is all radial (φ,ρ) satisfying

$$\begin{cases} -\Delta\varphi(r) = \rho(r), & \text{(5.1a)} \\ \operatorname{div}\big(\rho(r)\nabla\varphi(r)\big) = 0, & \text{(5.1b)} \\ \varphi(r = r_0) = 1, & \text{(5.1c)} \\ \varphi(r = 1) = 0, & \text{(5.1d)} \\ \dfrac{\partial \varphi}{\partial r}(r = r_0) = -A, & \text{(5.1e)} \end{cases}$$

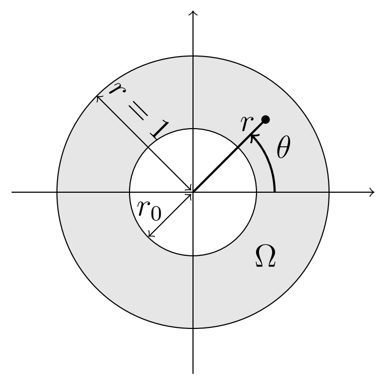

FIGURE 4. Definition domain in the radial case.

where A is a strictly positive constant. These solutions are given by the next theorem.

Theorem 5.1. *All but one radial solutions* (φ, ρ) *of the system* (5.1a)–(5.1d) *are given by:*

$$\varphi_\lambda(r) = \frac{F_\lambda(1) - F_\lambda(r)}{F_\lambda(1) - F_\lambda(r_0)}, \tag{5.2}$$

and

$$\rho_\lambda(r) = \begin{cases} \dfrac{\lambda}{(F_\lambda(1) - F_\lambda(r_0))\sqrt{1+\lambda r^2}} & \textit{if } \lambda \geqslant -1, \\ \dfrac{-\lambda}{(F_\lambda(1) - F_\lambda(r_0))\sqrt{-1-\lambda r^2}} & \textit{if } \lambda \leqslant \dfrac{-1}{r_0^2} < -1, \end{cases} \tag{5.3}$$

for $r_0 \leqslant r \leqslant 1$*, where* λ *is a real parameter varying in* $\left]-\infty, \frac{-1}{r_0^2}\right] \cup [-1, +\infty[$. *The function* $F_\lambda : [r_0, 1] \to \mathbb{R}$ *is increasing and defined as follows:*

$$F_\lambda(r) = \begin{cases} \sqrt{1+\lambda r^2} - \ln(\sqrt{1+\lambda r^2} + 1) + \ln(r) & \textit{if } \lambda \geqslant -1, \\ \sqrt{-\lambda r^2 - 1} - \arctan(\sqrt{-\lambda r^2 - 1}) & \textit{if } \lambda \leqslant \dfrac{-1}{r_0^2}. \end{cases} \tag{5.4}$$

The Neumann condition (5.1e) *is satisfied for the following value of* A*:*

$$A_\lambda := \frac{\sqrt{|\lambda + r_0^{-2}|}}{F_\lambda(1) - F_\lambda(r_0)}. \tag{5.5}$$

The remaining radial solution is:

$$\varphi_\infty(r) := \frac{1-r}{1-r_0}, \quad \rho_\infty(r) := \frac{1}{r(1-r_0)}, \quad \textit{with} \quad A_\infty := \frac{1}{1-r_0}.$$

Finally, for each $A \in [0, A_{-1}]$, *there is a unique solution* (φ, ρ) *to* (5.1a)–(5.1e) *and the maps*

$$[0, A_{-1}] \to H^1\big(]r_0, 1[\big) : A \mapsto \varphi_\lambda \text{ with } A_\lambda = A,$$
$$]0, A_{-1}[\to L^2\big(]r_0, 1[\big) : A \mapsto \rho_\lambda \text{ with } A_\lambda = A$$

are continuous.

In the previous Theorem, the electrostatic solution corresponds to $\lambda = 0$ and is given by:

$$\varphi_0(r) = \varphi_{\mathrm{e}}(r) = \frac{\ln(r)}{\ln(r_0)}. \tag{5.6}$$

In that case, the Neumann condition holds for A being $A_0 = -1/(r_0 \ln(r_0))$.

In Figure 5, the graph of the function $\lambda \mapsto A_\lambda$ is drawn which allows to visualize the relationship between λ and A.

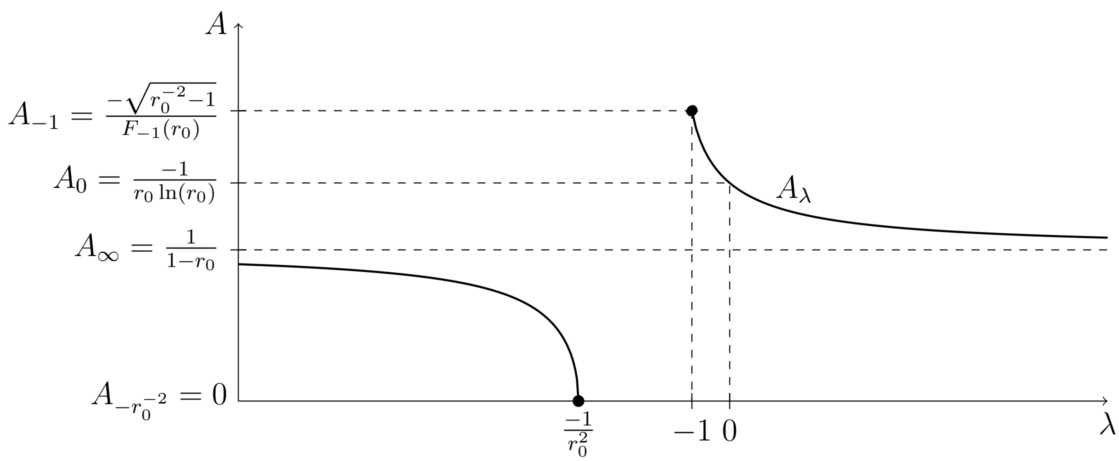

FIGURE 5. Graph of the function $\lambda \mapsto A_\lambda$.

Proof of Theorem 5.1. Let us start by computing all radial solutions to (5.1a)–(5.1e). Because φ and ρ are radial functions, Equations (5.1a) and (5.1b) become, respectively,

$$-\frac{\partial^2 \varphi}{\partial r^2}(r) - \frac{1}{r}\frac{\partial \varphi}{\partial r}(r) = \rho(r), \tag{5.7}$$

$$\frac{\partial}{\partial r}\Big(\rho(r)\frac{\partial \varphi}{\partial r}(r)\Big) + \frac{1}{r}\rho(r)\frac{\partial \varphi}{\partial r}(r) = 0. \tag{5.8}$$

The second equation is equivalent to the fact that there exists a real constant K such that

$$\forall r \in]r_0, 1[, \qquad \rho(r)\frac{\partial \varphi}{\partial r}(r) = \frac{K}{r}. \tag{5.9}$$

Multiplying (5.7) by $\partial\varphi/\partial r$ and using (5.9) yields

$$-\frac{\partial^2\varphi}{\partial r^2}(r)\frac{\partial\varphi}{\partial r}(r) - \frac{1}{r}\Big(\frac{\partial\varphi}{\partial r}(r)\Big)^2 = \frac{K}{r}. \tag{5.10}$$

This is equivalent to (5.7) provided that $(\partial\varphi/\partial r)(r) \neq 0$ for almost every $r \in \,]r_0, 1[$. Equation (5.10) can be seen as a linear equation in $(\partial\varphi/\partial r)^2$ and solving it implies that

$$\forall r \in \,]r_0, 1[, \qquad \Big(\frac{\partial\varphi}{\partial r}(r)\Big)^2 = \frac{\widetilde{K}}{r^2} - K \tag{5.11}$$

for some constant $\widetilde{K} \in \mathbb{R}$. It is not possible that K and $\widetilde{K}$ both vanish as that would imply that φ is constant and so cannot satisfy the boundary conditions (5.1c) and (5.1d). Therefore $\partial\varphi/\partial r$ vanishes at at most one point and so (5.11) is equivalent to (5.7). Depending on the value of $\widetilde{K}$, we can distinguish two cases.

1) **Case $\widetilde{K} = 0$.**
   Equality (5.11) says that $\partial\varphi/\partial r$ is constant and the boundary condition (5.1e) that $\partial\varphi/\partial r \equiv -A$ and $A^2 = -K$. Hence, using (5.1d),

$$\varphi(r) = \int_r^1 A \,\mathrm{d}s = A(1 - r).$$

   The boundary condition (5.1c) leads to

$$A = A_\infty \coloneqq \frac{1}{1 - r_0},$$

   and so $\varphi(r) = \frac{1-r}{1-r_0}$. Now using (5.9) and $K = -A^2$, we get $\rho(r) = \frac{1}{r(1-r_0)}$.

2) **Case $\widetilde{K} \neq 0$.**
   Let us set $\lambda \coloneqq -K/\widetilde{K}$. Equality (5.11) thus becomes

$$\forall r \in \,]r_0, 1[, \qquad \Big(\frac{\partial\varphi}{\partial r}(r)\Big)^2 = \widetilde{K}(r^{-2} + \lambda). \tag{5.12}$$

   If the right hand side vanishes in $]r_0, 1[$, it changes sign and so $\partial\varphi/\partial r$ will not be defined on the whole $]r_0, 1[$. Therefore $\widetilde{K}(r^{-2} + \lambda) > 0$ for all $r \in \,]r_0, 1[$ or, equivalently, $\lambda \geqslant -1$ if $\widetilde{K} > 0$ and $\lambda \geqslant -r_0^{-2}$ if $\widetilde{K} < 0$. Given the boundary conditions (5.1c) and (5.1d), $\partial\varphi/\partial r$ must be negative at some $r \in \,]r_0, 1[$, so

$$\frac{\partial\varphi}{\partial r}(r) = -\sqrt{\widetilde{K}(r^{-2} + \lambda)} \tag{5.13}$$

   and, using (5.1d), we get

$$\varphi(r) = \int_r^1 \sqrt{\widetilde{K}(s^{-2} + \lambda)}\,\mathrm{d}s.$$

   Distinguishing the cases $\widetilde{K} > 0$ and $\widetilde{K} < 0$, we find after integration that

$$\varphi(r) = \sqrt{|\widetilde{K}|}\big(F_\lambda(1) - F_\lambda(r)\big) \tag{5.14}$$

where F_λ is defined in the statement of the theorem. Imposing the boundary condition (5.1c) enables to determine $\sqrt{|\widetilde{K}|}$ and then to rewrite (5.14) as

$$\varphi_\lambda(r) = \frac{F_\lambda(1) - F_\lambda(r)}{F_\lambda(1) - F_\lambda(r_0)}. \tag{5.15}$$

It remains to impose condition (5.1e). In view of (5.13), it is equivalent to $A = \sqrt{\widetilde{K}(r_0^{-2} + \lambda)}$ or, equivalently, given the value for $\sqrt{|\widetilde{K}|}$ found above,

$$A = A_\lambda := \frac{\sqrt{|\lambda + r_0^{-2}|}}{F_\lambda(1) - F_\lambda(r_0)}. \tag{5.16}$$

The expression (5.3) for ρ follows from (5.9), (5.13) and $\lambda = -K/\widetilde{K}$.
To prove uniqueness of the radial solution, it remains to establish that the map $\mathcal{A} : \lambda \mapsto A_\lambda$ is one-to-one on $\lambda \in \,]-\infty, -r_0^{-2}] \cup [-1, +\infty[\cup \{\infty\}$. To that end, it suffices to prove that $\mathcal{A}$ is decreasing on $]-\infty, -r_0^{-2}]$ and on $[-1, +\infty[$ and that $A_\lambda \to A_\infty$ as $\lambda \to \pm\infty$. Note that, since $\mathcal{A}$ is obviously continuous on $]-\infty, -r_0^{-2}] \cup [-1, +\infty[$ in view of (5.4) and (5.16), this also implies that the image of $\mathcal{A}$ is $[A_{-r_0^{-2}}, A_\infty[\cup]A_\infty, A_{-1}] \cup \{A_\infty\} = [0, A_{-1}]$. Consequently, the inverse of $\mathcal{A}$,

$$\mathcal{A}^{-1} : [0, A_{-1}] \to \operatorname{Dom} \mathcal{A} : A \mapsto \lambda \text{ such that } A_\lambda = A$$

is continuous when $\operatorname{Dom} \mathcal{A}$ is seen as the three pieces $[-r_0^{-2}, -\infty[$, $\{\infty\}$, and $]+\infty, -1]$ glued together with the topology coming from the compactification of $\mathbb{R}$ with a single point at infinity.

Let now show that $\mathcal{A}$ is decreasing by showing that $\partial_\lambda A_\lambda < 0$ on $]-\infty, r_0^{-2}[\cup]-1, +\infty[$. Thanks to (5.16),

$$\frac{1}{A_\lambda} = \frac{F_\lambda(1) - F_\lambda(r_0)}{\sqrt{|\lambda + r_0^{-2}|}} = \frac{r_0}{\sqrt{1 + \lambda r_0^2}} \int_{r_0}^1 \frac{1}{s} \sqrt{|1 + \lambda s^2|}\, \mathrm{d}s = \int_{r_0}^1 \frac{r_0}{s} \sqrt{\frac{1 + \lambda s^2}{1 + \lambda r_0^2}}\, \mathrm{d}s.$$

A direct computation yields,

$$\partial_\lambda \left(\frac{r_0}{s} \sqrt{\frac{1 + \lambda s^2}{1 + \lambda r_0^2}} \right) = \frac{r_0}{2s} \sqrt{\frac{1 + \lambda r_0^2}{1 + \lambda s^2}} \frac{s^2 - r_0^2}{(1 + \lambda r_0^2)^2}.$$

Since $s^2 - r_0^2 > 0$ for $s \in \,]r_0, 1]$, one deduces

$$\partial_\lambda \left(\frac{1}{A_\lambda} \right) = -\frac{\partial_\lambda A_\lambda}{A_\lambda^2} > 0,$$

whence the claim.

Let us now turn to the limits as $\lambda \to \pm\infty$. Using l'Hôpital's rule and (5.4), it is straightforward to show that $F_\lambda(r)/\sqrt{\lambda} \to r$ as $\lambda \to +\infty$ and $F_\lambda(r)/\sqrt{-\lambda} \to r$ as $\lambda \to -\infty$. The fact that $A_\lambda \to A_\infty$ as $\lambda \to \pm\infty$ then readily follows from (5.16).

Finally, it remains to prove that the maps

$$\operatorname{Dom} \mathcal{A} \to H^1(]r_0, 1[) : \lambda \mapsto \varphi_\lambda, \qquad \operatorname{Dom} \mathcal{A} \setminus \left\{ \frac{-1}{r_0^2}, -1 \right\} \to L^2(]r_0, 1[) : \lambda \mapsto \rho_\lambda$$

(with the above described topology on Dom $\mathcal{A}$) are continuous. This results from the explicit expressions (5.13) and (5.15) for φ_λ and (5.3) for ρ_λ. When $\lambda \to \pm\infty$, we divide both the numerator and denominator by $\sqrt{|\lambda|}$. □

Since we have fixed $\varphi = 1$ on Γ_c, a solution (φ, ρ) is said to be *physical* if $\rho \geqslant 0$. In view of (5.3), $(\varphi_\lambda, \rho_\lambda)$ is physical if and only if $\lambda \in \,]-\infty, -r_0^{-2}] \cup [0, +\infty[\, \cup \{\infty\}$. Figure 6 illustrates these results for $r_0 = 0.25$. On the contrary, for $\lambda \in [-1, 0[$, the solutions are nonphysical because $\rho_\lambda < 0$ (see Figure 7). Note that, when $\lambda = -1/r_0^2$ (resp. $\lambda = -1$), ρ_λ is singular at $r = r_0$ (resp. $r = 1$) and does not belong to $L^2(]r_0, 1[)$; see Figures 6b and 7b for an illustration.

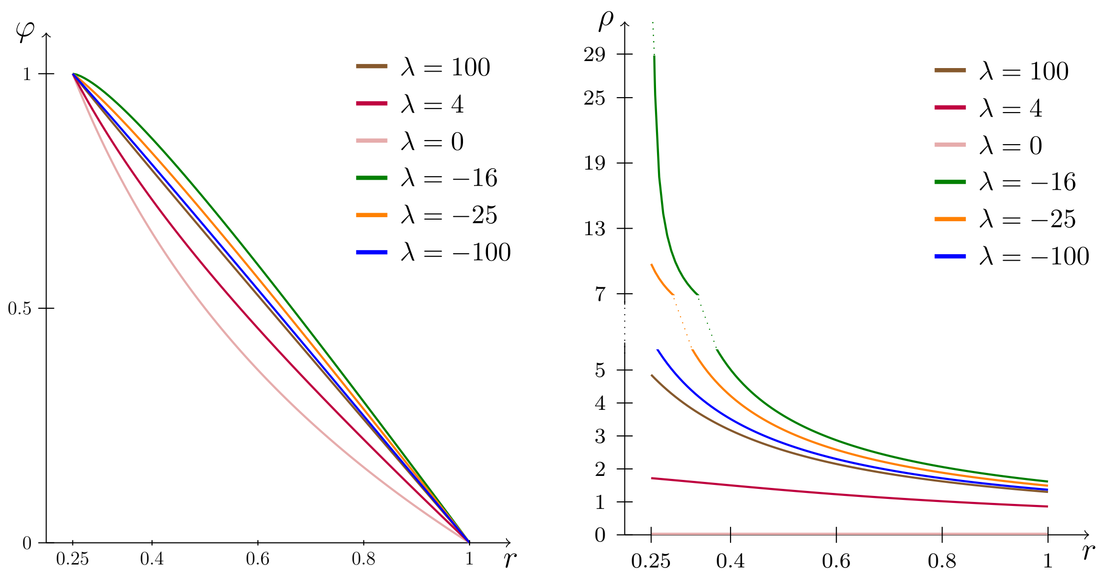

(A) Electrical potential φ.   (B) Charge density ρ.

FIGURE 6. Physical radial solutions for $r_0 = 0.25$ and different values of λ.

Furthermore, Figures 6 and 7 enable us to visualize the continuous dependence of solutions (φ, ρ) with respect to A which was mentioned in the statement of Theorem 5.1.

Remark 5.2. Solutions of the system (5.1a)–(5.1e) in the case $\lambda \geqslant 0$ were already given without proof in [7, Appendix A], [18, formula (8)], [21, Appendix B], and [22]. Here, we provide an exhaustive determination of (physical) radial solutions and demonstrate that the set of solutions as A changes forms a continuum.

6. A Least-Square Algorithm

In section 3, we proved the existence of solutions to (3.1) by adding a small diffusion term, $\varepsilon\Delta\rho$, and letting ε tends to zero. While this approach may be turned into an

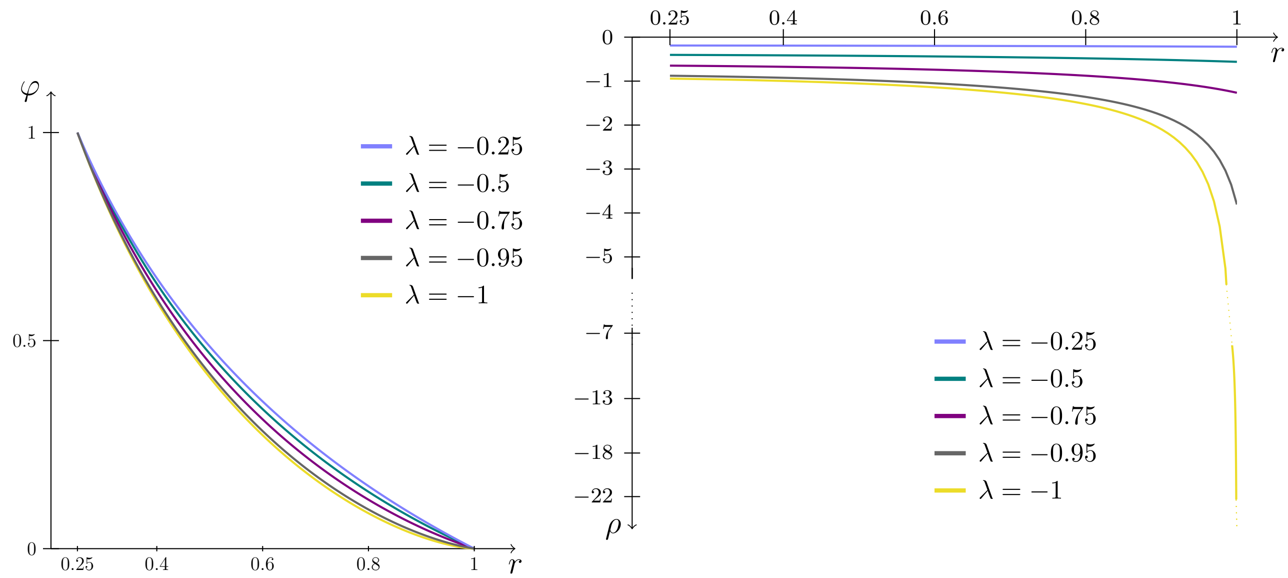

(A) Non-physical solution φ.

(B) Non-physical solution ρ.

FIGURE 7. Non-physical radial solution for $r_0 = 0.25$ and different values of λ

algorithm, there are two issues. Firstly, there is no good computational counterpart to the Schauder fixed point theorem. The second issue concerns the Neumann boundary condition in (1.2). This condition cannot be controlled using this approach, even though it is important for the engineers to be able to specify it. In this section, we present a least squares approach to solving (1.1)–(1.2) that relies solely on the classical Finite Element Method (FEM).

Let us start by noticing that we can equivalently write the second equation of (1.1) as $-\operatorname{div}\big((\rho+1)\nabla\varphi\big) = \rho$. The advantage of this form is that, since ρ can tend to 0 (see [12, Section 1]), the ellipticity of the linear operator is kept. Moreover, the constant of ellipticity is bounded away of 0 independently of ρ. In summary, we here want to compute a numerical approximation of the solution (φ, ρ) to the problem

$$\begin{cases} -\Delta\varphi = \rho, & \text{in } \Omega, \\ -\operatorname{div}\big((\rho+1)\nabla\varphi\big) = \rho, & \text{in } \Omega, \\ \varphi = 1, & \text{on } \Gamma_{\mathrm{c}}, \\ \varphi = 0, & \text{on } \Gamma_{\mathrm{d}}, \\ \dfrac{\partial\varphi}{\partial\boldsymbol{n}} = A, & \text{on } \Gamma_{\mathrm{c}}, \end{cases} \tag{6.1}$$

where A may be a constant or a sufficiently smooth function.

6.1. **Description of the algorithm.** For a fixed function ρ, we divide the system (6.1) into two subsystems with unknowns φ_1 and φ_2 (below they will be denoted by

$\varphi_1(\rho)$ and $\varphi_2(\rho)$ to emphasize their dependency with respect to ρ):

$$\begin{cases} -\Delta\varphi_1 = \rho, & \text{in } \Omega,\\ \dfrac{\partial\varphi_1}{\partial \boldsymbol{n}} = A, & \text{on } \Gamma_{\rm c},\\ \varphi_1 = 0, & \text{on } \Gamma_{\rm d}, \end{cases} \tag{6.2}$$

and

$$\begin{cases} -\operatorname{div}\big((\rho+1)\nabla\varphi_2\big) = \rho, & \text{in } \Omega,\\ \varphi_2 = 1, & \text{on } \Gamma_{\rm c},\\ \varphi_2 = 0, & \text{on } \Gamma_{\rm d}. \end{cases} \tag{6.3}$$

Note that both problems have a unique solution in $H^1(\Omega)$ as soon as A belongs to $H^{1/2}(\Gamma_{\rm c})$, $\rho \in L^\infty(\Omega)$, and $\rho \geqslant 0$, thanks to Lax-Milgram theorem. Then, we introduce the functional

$$J : L^\infty(\Omega) \to \mathbb{R} : \rho \mapsto \tfrac{1}{2}\big\|\nabla\big(\varphi_1(\rho) - \varphi_2(\rho)\big)\big\|_\Omega^2, \tag{6.4}$$

and notice that $J(\rho)$ vanishes if and only if $\varphi_1(\rho) = \varphi_2(\rho)$ which means that $(\varphi_1(\rho), \rho)$ is a solution to (6.1).

The FEM is used to discretize both equations, (6.2) and (6.3). To give additional details, let us fix $V_h(\Omega)$ a finite-dimensional subspace of $H^1(\Omega) \cap L^\infty(\Omega)$ and $V_{h,\Gamma_{\rm d}}(\Omega) \coloneqq \{u_h \in V_h(\Omega) \mid u_h = 0 \text{ on } \Gamma_{\rm d}\}$, both equipped with the H^1-norm. Let $\rho_h \in V_h(\Omega)$ be such that $\rho_h \geqslant 0$. The variational formulation of the discrete approximation of (6.2) consists in finding $\varphi_{1,h} \in V_{h,\Gamma_{\rm d}}(\Omega)$ such that

$$\forall \chi \in V_{h,\Gamma_{\rm d}}(\Omega), \qquad \int_\Omega \nabla\varphi_{1,h}\nabla\chi \,\mathrm{d}x = \int_\Omega \rho_h\chi\,\mathrm{d}x + \int_{\Gamma_{\rm c}} A\chi\,\mathrm{d}x. \tag{6.5}$$

We proceed similarly for (6.3). Let $V_{h,\partial\Omega}(\Omega) \coloneqq \{u_h \in V_h(\Omega) \mid u_h = 0 \text{ on } \partial\Omega\}$. The variational form of (6.3) consists in seeking $\varphi_{2,h} \in V_{h,\Gamma_{\rm d}}(\Omega)$ such that $\varphi_{2,h} = 1$ on $\Gamma_{\rm c}$ and

$$\forall \chi \in V_{h,\partial\Omega}(\Omega), \qquad \int_\Omega (\rho_h + 1)\nabla\varphi_{2,h}\nabla\chi\,\mathrm{d}x = \int_\Omega \rho_h\chi\,\mathrm{d}x. \tag{6.6}$$

The discrete version of functional J defined by (6.4) is given by

$$J_h : V_h(\Omega) \to \mathbb{R} : \rho_h \mapsto \tfrac{1}{2}\big\|\nabla\big(\varphi_{1,h}(\rho_h) - \varphi_{2,h}(\rho_h)\big)\big\|_\Omega^2.$$

In order to minimize J_h, we want to calculate its gradient $\nabla J_h \in V_h(\Omega)$ with respect to the H^1-topology, which is characterized as follows. For any $z \in V_h(\Omega)$,

$$\begin{aligned} \big(\nabla J_h(\rho_h) \bigm| z\big)_{H^1} &= \frac{\partial J_h}{\partial \rho_h}(\rho_h)[z]\\ &= \big(\nabla(\varphi_{1,h} - \varphi_{2,h}) \bigm| \nabla\big(\partial_{\rho_h}(\varphi_{1,h} - \varphi_{2,h})[z]\big)\big)_\Omega\\ &= \big(\nabla(\varphi_{1,h} - \varphi_{2,h}) \bigm| \nabla(\varphi'_{1,h,z} - \varphi'_{2,h,z})\big)_\Omega, \end{aligned} \tag{6.7}$$

where $\varphi'_{1,h,z} := \partial_{\rho_h}\varphi_{1,h}[z]$ and $\varphi'_{2,h,z} := \partial_{\rho_h}\varphi_{2,h}[z]$. To compute $\varphi'_{1,h,z}$ and $\varphi'_{2,h,z}$, we differentiate Equations (6.5) and (6.6) with respect to ρ_h in the direction z. We then obtain the following two equations:

$$\forall \chi \in V_{h,\Gamma_\mathrm{d}}(\Omega), \qquad \int_\Omega \nabla\varphi'_{1,h,z}\nabla\chi\,\mathrm{d}x = \int_\Omega z\chi\,\mathrm{d}x, \tag{6.8}$$

where $\varphi'_{1,h,z} \in V_{h,\Gamma_\mathrm{d}}(\Omega)$ and

$$\forall \chi \in V_{h,\partial\Omega}(\Omega), \qquad \int_\Omega (\rho_h + 1)\nabla\varphi'_{2,h,z}\nabla\chi\,\mathrm{d}x = \int_\Omega z\chi - z\nabla\varphi_{2,h}\nabla\chi\,\mathrm{d}x, \tag{6.9}$$

where $\varphi'_{2,h,z} \in V_{h,\partial\Omega}(\Omega)$.

We now want to rewrite the right hand side of Equality (6.7) in order to not to have to compute it for a basis of z. For the part involving $\varphi'_{1,h,z}$, we have

$$\begin{aligned}\big(\nabla(\varphi_{1,h} - \varphi_{2,h}) \mid \nabla\varphi'_{1,h,z}\big)_\Omega &= \int_\Omega \nabla(\varphi_{1,h} - \varphi_{2,h})\nabla\varphi'_{1,h,z}\,\mathrm{d}x \\ &= \int_\Omega (\varphi_{1,h} - \varphi_{2,h})z\,\mathrm{d}x = \big(\varphi_{1,h} - \varphi_{2,h} \mid z\big)_\Omega \quad \text{by (6.8)}.\end{aligned}$$

For the second part, we introduce the intermediate function $\Psi_h \in V_{h,\partial\Omega}(\Omega)$ which is the solution to the following variational problem:

$$\forall \chi \in V_{h,\partial\Omega}(\Omega), \qquad \int_\Omega (\rho_h + 1)\nabla\Psi_h\nabla\chi\,\mathrm{d}x = \int_\Omega \nabla(\varphi_{1,h} - \varphi_{2,h})\nabla\chi\,\mathrm{d}x. \tag{6.10}$$

Hence, we have:

$$\begin{aligned}\big(\nabla(\varphi_{1,h} - \varphi_{2,h}) \mid \nabla\varphi'_{2,h,z}\big)_\Omega &= \int_\Omega \nabla(\varphi_{1,h} - \varphi_{2,h})\nabla\varphi'_{2,h,z}\,\mathrm{d}x \\ &= \int_\Omega (\rho_h + 1)\nabla\Psi_h\nabla\varphi'_{2,h,z}\,\mathrm{d}x \qquad \text{by (6.10)} \\ &= \int_\Omega z\Psi_h - z\nabla\varphi_{2,h}\nabla\Psi_h\,\mathrm{d}x \qquad \text{by (6.9)} \\ &= \big(\Psi_h - \nabla\varphi_{2,h}\nabla\Psi_h \mid z\big)_\Omega.\end{aligned}$$

The last identities allow to simplify the equation (6.7) for $\nabla J_h(\rho_h) \in V_h(\Omega)$ into

$$\forall z \in V_h(\Omega), \quad \big(\nabla J_h(\rho_h) \mid z\big)_{H^1} = \big(\varphi_{1,h} - \varphi_{2,h} - \Psi_h + \nabla\varphi_{2,h}\nabla\Psi_h \mid z\big)_\Omega. \tag{6.11}$$

Algorithm. *For the algorithm, we have created four subroutines as follows: given $\rho \in V_h(\Omega)$, we can*

(1) Compute the solution $\varphi_{1,h}(\rho_h)$ to (6.5) using the FEM.
(2) Compute the solution $\varphi_{2,h}(\rho_h)$ to (6.6) with the FEM.
(3) Compute the functional $J_h(\rho_h)$ with $\varphi_{1,h}(\rho_h)$ and $\varphi_{2,h}(\rho_h)$.
(4) Compute $\nabla J_h(\rho_h)$ by solving Equation (6.11) with the FEM, the quantities $\varphi_{1,h}(\rho_h)$ and $\varphi_{2,h}(\rho_h)$ being computed using the above subroutines and Ψ_h being the solution to (6.10), computed again with the FEM.

Given a tolerance `tol` *(by default* 10^{-12}*), a maximum number of iterations* `N` *(by default* 500*) and an initial guess* $\rho_0 \in V_h(\Omega)$*, we use a minimization algorithm that stops when* $J_h(\rho_h) \leqslant$ `tol` *or the maximum number of iterations exceeds* `N`*.*

6.2. **Some additional numerical details.** The Finite Element Method, used to compute the functions $\varphi_{1,h}$ and $\varphi_{2,h}$, is implemented via the Python library *Netgen* [19]. Here we choose $V_h(\Omega)$ to be the space of P1 elements. For the minimization step, we use the *Scipy* library, and more specifically its function *scipy.optimize.minimize*, which provides access to several optimization algorithms. Among these, we selected only methods that require the gradient of the objective function but not the explicit computation of the Hessian matrix.

Of those routines, the L-BFGS-B one is significantly the faster but exhibits convergence problems depending on the version of Scipy used. In the latest version, the method fails due to a known unresolved bug [16]. In earlier version, we observed some abnormal terminations when applying L-BFGS-B to the Rosenbrock function. The SLSQP method is the slowest of all those tested (up to 50 times slower).

The remaining two methods, namely Trust Constraint (trust-constr) and Conjugate Gradient (CG), are the fastest and converge to the default tolerance of the functional J_h across a variety of test cases. They are essentially on par in terms of speed and precision. The numerical tests below were performed using trust-constr.

6.3. **Numerical results.**

6.3.1. *Radial case.* Since analytical solutions are available for the radial case, we first test our algorithm in this setting to check whether it converges to the exact solution. We take the radius of the interior boundary, r_0, as 0.25 (see Figure 4) and the Neumann condition is given by formula (5.5) with $\lambda = -50$. Starting with the initial density $\rho_0(x, y) := x^2 + y^2 + 1$, we let the algorithm converges for various mesh sizes. Figure 8 shows, in a double logarithmic scale, the relative error between φ_{exact}, the exact solution φ given by (5.2), and φ_{num}, the approximate solution φ computed numerically, in blue. The same figure shows, in red, the relative error between ρ_{exact}, the exact solution ρ given by (5.3), and ρ_{num}, the approximate solution ρ computed numerically. Both errors decrease to zero as the mesh size $h \to 0$. This provides evidence that, in that specific case, the numerical solution approaches the exact one with an error of order of about $h^{1.66}$ for φ and $h^{2.33}$ for ρ.

To shed some light on the size of the basin of convergence, we ran the algorithm with different initial densities ρ_0 on a mesh with a size $h \approx 3 \cdot 10^{-2}$ (2690 degrees of freedom). For the above choice of ρ_0, the initial value of J_h is $3.6 \cdot 10^{-6}$ and the default tolerance of 10^{-12} is reached after 152 iterations. For the nonradial $\rho_0(x, y) = x^2 + 100$, the initial value of J_h is approximately 430 and the algorithm reaches the default tolerance after 157 iterations. We have also tried several additional initial ρ_0, for example one that oscillates in the polar angle, $\rho_0(x, y) = 1 + y/\sqrt{x^2 + y^2}$, and the results are sensibly the same in all cases. This highlights the robustness of the algorithm with respect to the initial guess.

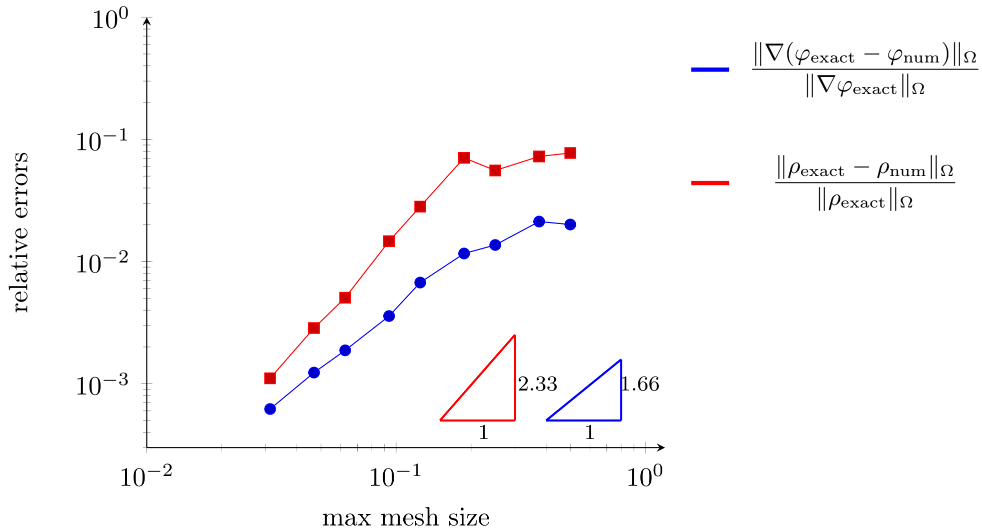

FIGURE 8. Convergence in the radial case to the exact solutions.

In section 5, all radial solutions were determined. A natural question is whether nonradial solutions exist for some boundary data $A : \Gamma_c \to \mathbb{R}$. Unfortunately, the results of section 3 do not provide an answer to that question. As an element of evidence towards a positive answer, we chose the nonradial $A(x, y) = \frac{1}{2} + \frac{1}{4}x/\sqrt{x^2 + y^2}$ (the constraint (4.3), with $\partial\varphi_e/\partial\boldsymbol{n}$ readily computed from (5.6), is satisfied), the initial guess $\rho_0(x, y) = x^2 + y^2 + 1$ and ran our algorithm. It converged with a final value for J_h of approximately $8.5 \cdot 10^{-13}$, suggesting that a nonradial solution indeed exists. The level curves of the final φ and ρ are depicted in Figure 9.

Finally, as we can see in the previous section 5, there does not exist a solution for A greater than A_{-1}. So, in that case, the algorithm should not converge. To exemplify this, let us take $A = 5$ and $\rho_0 = x^2 + y^2 + 1$. The algorithm stops because the default number of iterations is exceeded and the final value of J_h is approximately 1.9, which is not small enough to consider the returned (φ, ρ) to be a solution.

6.3.2. *The unipolar half-disk.* Now, let us consider a more general case for which exact solutions cannot be computed analytically. More precisely, we consider the case of a half-disk containing a circular conductor (see Figure 1). The radius of the interior circle centered at $(0, 0)$ (i.e. the interior boundary) has been chosen to be 0.25. The center of the exterior circle is at the point $(0, -1)$ and its radius is 2. Since we only consider the half-disk, the coordinates of its corners are $(-2, -1)$ and $(2, -1)$.

As we did for the radial case, we have tested different initial guesses ρ_0 and different values for the Neumann condition A. We performed our tests with a mesh of size $h = 5 \cdot 10^{-2}$ (2784 degrees of freedom). First, we considered the initial guess $\rho_0(x, y) = \sqrt{x^2 + y^2} + 1$ and the Neumann condition $A = 1$ and we numerically verified that the constraint (4.3) is satisfied. In Figure 10, we can see the level curves of the solution (φ, ρ). We can note that the value for ρ is higher around the interior boundary. This makes sense physically because ρ represents the space charges in the air that

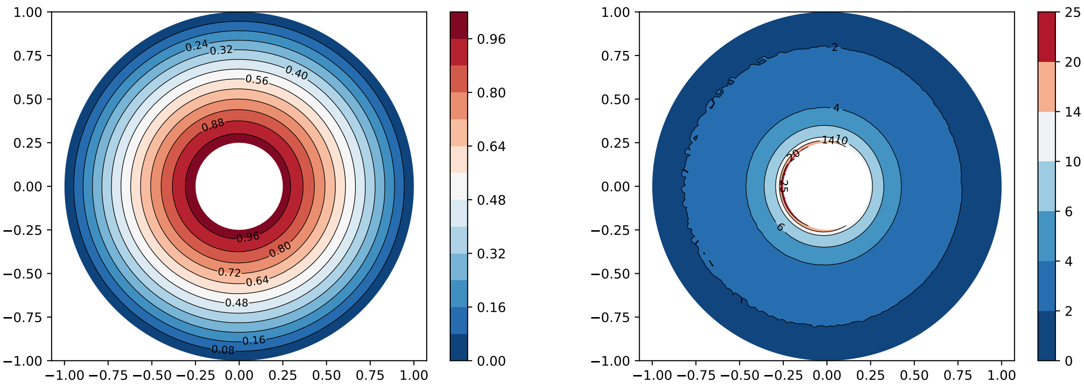

FIGURE 9. Levels curves for the numerical solutions φ (left) and ρ (right) with $A(x, y) = \frac{1}{2} + \frac{1}{4}x/\sqrt{y^2 + x^2}$.

in practice are higher near the conductor. We also observe that ρ goes to zero near the corners. As in the previous section, the algorithm keep converging (to the same solution) when starting with different initial guesses more distant from the solution (i.e. with higher values of J_h).

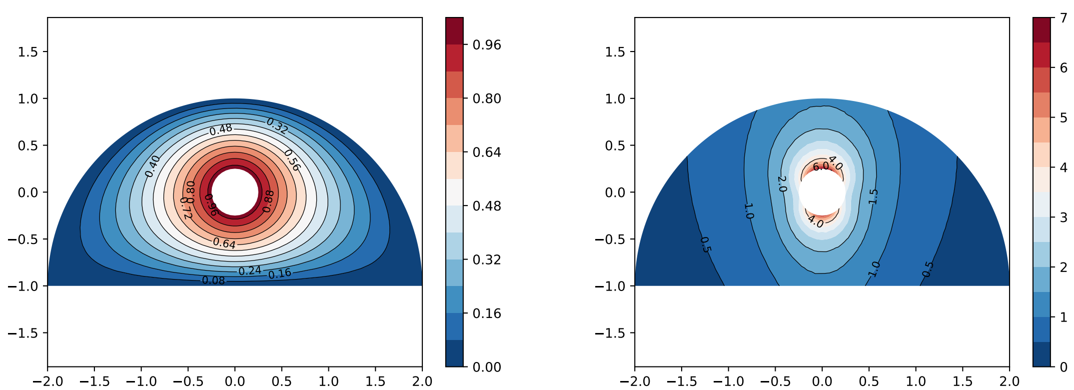

FIGURE 10. Levels curves for φ (left) and ρ (right) with $A = 1$.

We also again tested the convergence of the algorithm for non-constant A's. As an example, for $A(x, y) = x/2 + 0.5$ and $\rho_0(x, y) = \sqrt{x^2 + y^2} + 1$, the algorithm reaches the default tolerance after 56 iterations. The final value of J_h is approximately $9.16 \cdot 10^{-13}$, suggesting that such a solution exists. We can see on Figure 11 the level curves of the solution (φ, ρ).

Finally, for a value of A greater than $\partial\varphi_e/\partial\boldsymbol{n}$ (see Theorem 4.1), the algorithm should not converge. To exemplify this, let us take $A = 3$ and $\rho_0 = \sqrt{x^2 + y^2} + 1$. The algorithm stops because the default maximum number of iterations is exceeded

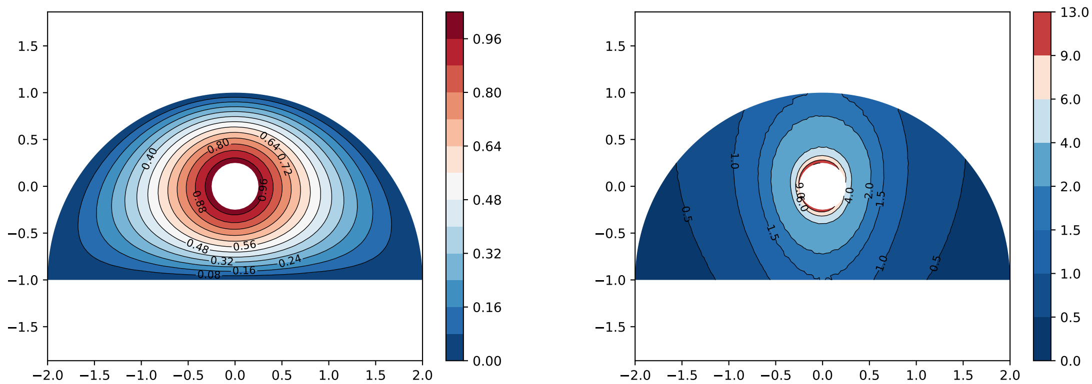

FIGURE 11. Levels curves for φ (left) and ρ (right) with $A(x, y) = x/2 + 0.5$.

and the final value of J_h is approximately $4.32 \cdot 10^{-3}$, which is not small enough to consider the returned (φ, ρ) to be a solution.

Remark 6.1. In these experiments, we consider simplified test cases which allow for an initial evaluation of the algorithm's performance. Although these cases are not representative of realistic physical scenarios, extending the approach to more representative configurations is part of our future work.

Acknowledgements

We are grateful to Prof. Stéphane Clénet (ENSAM Lille, France) for introducing us to the topic of HVDC transport, for his invaluable help on the physical aspects of the problem, as well as for his enthusiastic support of our findings. We also would like to thank Zuqi Tang (L2EP Lille, France) for interesting discussions and for his involvement in the supervision of Madeline Chauvier's PhD thesis.

References

[1] C. K. Arruda and A. C. Lima. "Corona modeling in HVDC transmission lines based on a modified particle-in-cell approach". In: *Electric Power Systems Research* 125 (2015), pp. 91–99. ISSN: 0378-7796. DOI: `https://doi.org/10.1016/j.epsr.2015.03.028`. URL: `https://www.sciencedirect.com/science/article/pii/S0378779615000954`.

[2] M. P. Bahrman and B. K. Johnson. "The ABCs of HVDC transmission technologies". In: *IEEE Power and Energy Magazine* 5.2 (2007), pp. 32–44. DOI: `10.1109/MPAE.2007.329194`.

[3] A. Butler, Z. Cendes, and J. Hoburg. "Interfacing the finite-element method with the method of characteristics in self-consistent electrostatic field models". In: *Industry Applications, IEEE Transactions on* 25 (June 1989), pp. 533 –538. DOI: `10.1109/28.31225`.

[4] S. Cristina, G. Dinelli, and M. Feliziani. "Numerical computation of corona space charge and V-I characteristic in DC electrostatic precipitators". In: *Industry Applications, IEEE Transactions on* 27 (Feb. 1991), pp. 147 –153. DOI: 10.1109/28.67546.

[5] D. Gilbarg and N. Trudinger. *Elliptic Partial Differential Equations of Second Order*. Classics in Mathematics. Springer Berlin Heidelberg, 2001. ISBN: 9783540411604. URL: https://books.google.be/books?id=eoiGTf4cmhwC.

[6] P. Grisvard. *Elliptic Problems in Nonsmooth Domains*. Society for Industrial and Applied Mathematics, 2011. DOI: 10.1137/1.9781611972030. eprint: https://epubs.siam.org/doi/pdf/10.1137/1.9781611972030. URL: https://epubs.siam.org/doi/abs/10.1137/1.9781611972030.

[7] W. Janischewskyj and G. Cela. "Finite element solution for electric fields of coronating dc transmission lines". In: *IEEE Transactions on Power Apparatus and Systems* 98.3 (1979), pp. 1000–1008.

[8] W. Janischewskyj and G. Cela. "Finite Element Solution for Electric Fields of Coronating DC Transmission Lines". In: *IEEE Transactions on Power Apparatus and Systems* PAS-98.3 (1979), pp. 1000–1012. DOI: 10.1109/TPAS.1979.319258.

[9] F. Lattarulo and V. Amoruso. *Filamentary ion flow : theory and experiments*. Wiley-IEEE Press, Jan. 2014, pp. 1–204.

[10] Z. Li and X. Zhao. "Calculation of Ion Flow Field of Monopolar Transmission Line in Corona Cage Including the Effect of Wind". In: *Energies* 12.20 (2019). ISSN: 1996-1073. DOI: 10.3390/en12203924. URL: https://www.mdpi.com/1996-1073/12/20/3924.

[11] J. Lobry. "A New Numerical Scheme for the Simulation of Corona Fields". In: *Magnetics, IEEE Transactions on* 50 (Feb. 2014), pp. 541–544. DOI: 10.1109/TMAG.2013.2281999.

[12] R. Magnanini, S. Nicaise, and M. Chauvier. "Critical points of solution of elliptic equations in divergence form in planar non simply connected domains with smooth or nonsmooth boundary". submitted. 2025.

[13] P. A. Markowich. *The stationary semiconductor device equations*. Computational Microelectronics. Springer-Verlag, Vienna, 1986, pp. ix+193. ISBN: 3-211-81892-8. DOI: 10.1007/978-3-7091-3678-2. URL: https://doi-org.proxybmath.univ-lille.fr/10.1007/978-3-7091-3678-2.

[14] T. W. May, Y. M. Yeap, and A. Ukil. "Comparative evaluation of power loss in HVAC and HVDC transmission systems". In: *2016 IEEE Region 10 Conference (TENCON)*. 2016, pp. 637–641. DOI: 10.1109/TENCON.2016.7848080.

[15] K. Meah and S. Ula. "Comparative Evaluation of HVDC and HVAC Transmission Systems". In: *2007 IEEE Power Engineering Society General Meeting*. 2007, pp. 1–5. DOI: 10.1109/PES.2007.385993.

[16] S. Müller. *BUG: optimize: worse behaviour of new L-BFGS-B implementation*. 2025. URL: https://github.com/scipy/scipy/issues/23161 (visited on 10/01/2025).

[17] Y. Park et al. "Fully Coupled Finite Element Analysis for Ion Flow Field Under HVDC Transmission Lines Employing Field Enhancement Factor". In: *IEEE Transactions on Power Delivery* 33.6 (2018), pp. 2856–2863. DOI: 10.1109/TPWRD.2018.2854678.

[18] M. P. Sarma and W. Janischewskyj. "Analysis of Corona Losses on DC Transmission Lines: I - Unipolar Lines". In: *IEEE Transactions on Power Apparatus and Systems* PAS-88.5 (1969), pp. 718–731. DOI: 10.1109/TPAS.1969.292362.

[19] J. Schöberl. *Netgen/NGSolve*. https://ngsolve.org/. 2022.

[20] U. Straumann and C. M. Franck. "Ion-Flow Field Calculations of AC/DC Hybrid Transmission Lines". In: *IEEE Transactions on Power Delivery* 28.1 (2013), pp. 294–302. DOI: 10.1109/TPWRD.2012.2214793.

[21] T. Takuma, T. Ikeda, and T. Kawamoto. "Calculation of ion flow fields of hvdc transmission lines by the finite element method". In: *IEEE Transactions on Power Apparatus and Systems* 100.12 (1981), pp. 4802–4810.

[22] J. S. Townsend. "The potentials required to maintain currents between coaxial cylinders". In: *Philosophical Magazine Series 6* 28.163 (1987), pp. 83–90.

[23] G. M. Troianiello. *Elliptic differential equations and obstacle problems*. The University Series in Mathematics. Plenum Press, New York, 1987, pp. xiv+353. ISBN: 0-306-42448-7. DOI: 10.1007/978-1-4899-3614-1. URL: https://doi-org.proxybmath.univ-lille.fr/10.1007/978-1-4899-3614-1.

[24] H. Wang. "Comparison and Analysis of Advantages and Disadvantages Based on UHV AC/DC Transmission". In: 2019. URL: https://api.semanticscholar.org/CorpusID:181840816.

[25] H. Wang and M. Redfern. "The advantages and disadvantages of using HVDC to interconnect AC networks". In: *45th International Universities Power Engineering Conference UPEC2010*. 2010, pp. 1–5.

[26] L. Xiu et al. "Analysis and Computation of Total Electric Field Under UHVDC Transmission Lines With Drizzle Weather". In: *IEEE Transactions on Dielectrics and Electrical Insulation* 31.2 (2024), pp. 980–987. DOI: 10.1109/TDEI.2023.3346350.

[27] T. Zhu et al. "Ion flow field modelling based on lattice Boltzmann method and its mesh refinement". In: *IET Generation, Transmission and Distribution* 14 (Sept. 2020), pp. 4539–4546. DOI: 10.1049/iet-gtd.2020.0149.

[28] H. Zou. "Chapter 7 - Fixed Point Theory and Elliptic Boundary Value Problems". In: *Handbook of Differential Equations*. Ed. by M. Chipot. Vol. 6. Handbook of Differential Equations: Stationary Partial Differential Equations. North-Holland, 2008, pp. 503–583. DOI: https://doi.org/10.1016/S1874-5733(08)80024-1. URL: https://www.sciencedirect.com/science/article/pii/S1874573308800241.

(Madeline Chauvier) Université Polytechnique Hauts-de-France, CÉRAMATHS/DMATHS and FR CNRS 2037,F-59313 - Valenciennes Cedex 9 France and Département de Mathématique, Université de Mons, place du parc 20, B-7000 Mons, Belgium
Email address: Madeline.CHAUVIER@umons.ac.be

(Serge Nicaise) Université Polytechnique Hauts-de-France, CÉRAMATHS/DMATHS and FR CNRS 2037, F-59313 - Valenciennes Cedex 9 France
Email address: Serge.Nicaise@uphf.fr

(Christophe Troestler) Département de Mathématique, Université de Mons, place du parc 20, B-7000 Mons, Belgium
Email address: Christophe.TROESTLER@umons.ac.be

(Juliette Venel) Université Polytechnique Hauts-de-France, CÉRAMATHS/DMATHS and FR CNRS 2037, F-59313 - Valenciennes Cedex 9 France
Email address: Juliette.Venel@uphf.fr